Swiss Journal of Geosciences (2018) 111:117–131
https://doi.org/10.1007/s00015-017-0288-x

Holocene evolution of the Triftje- and the Oberseegletscher (Swiss Alps) constrained with ^{10}Be exposure and radiocarbon dating

Olivia Kronig[1] · Susan Ivy-Ochs[1] · Irka Hajdas[1] · Marcus Christl[1] · Christian Wirsig[1] · Christian Schlüchter[2]

Received: 19 August 2016 / Accepted: 24 November 2017 / Published online: 11 December 2017
© Swiss Geological Society 2017

Abstract
To develop a more precise understanding of Alpine glacier fluctuations during the Holocene, the glacier forefields of the Triftjegletscher and the Oberseegletscher east of Zermatt in the Valais Alps, Switzerland, were investigated. A multi-disciplinary approach of detailed geological and geomorphological field mapping combined with ^{10}Be exposure and radiocarbon dating was applied. A total of twelve samples of boulders and bedrock were taken from both Little Ice Age (LIA) landforms, as documented by the Dufour map published in 1862, and from landforms outside of the LIA. The resulting ^{10}Be ages range between 12590 ± 350 a and 420 ± 170 a. A piece of wood found embedded in the Little Ice Age moraine gave radiocarbon ages that range between 293 cal years BP up to modern (356–63 cal years before 2013). Based on these results, four tentative steps of the Holocene evolution could be distinguished. An early Holocene stage, which documents the decay of the Egesen stadial glaciers when the first parts of the study area became ice free. This was followed by a phase with no evidence of glacier advance. Then in the late Holocene, the glaciers advanced (at least) twice. An advance around 1200 a, as shown by several moraine ages, coincides with the Göschenen II cold phase. A more extensive readvance occurred during the LIA as shown on the historical maps and underpinned by one ^{10}Be exposure age and the radiocarbon age. This later advance destroyed or overprinted the earlier landforms in most parts of the area.

Keywords Glacier reconstruction · Cosmogenic ^{10}Be · Holocene · Little Ice Age · Göschenen II

1 Introduction

The current interglacial period, the Holocene, began 11.7 ka ago (Rasmussen et al. 2006). Over the course of the Holocene, glaciers in the Alps fluctuated markedly (Maisch et al. 1999, 2003; Nicolussi and Patzelt 2000a, b; Hormes et al. 2001; Deline and Orombelli 2005; Holzhauser et al. 2005; Nicolussi et al. 2005; Joerin et al. 2006, 2008; Kerschner and Ivy-Ochs 2008; Nicolussi and Schlüchter 2012; Schimmelpfennig et al. 2012, 2014; Heiri et al. 2014; Le Roy et al. 2015; Solomina et al. 2015) in response to climate variations punctuated by several short cold phases (Wanner et al. (2011) and references therein). The understanding of glacier histories allows to put recent retreats, in the context of Holocene climate variations (Schneebeli and Röthlisberger 1976; Holzhauser 1995, 2010; Maisch et al. 2003; Böhlert et al. 2011; Nicolussi and Schlüchter 2012; Schimmelpfennig et al. 2012; Hippe et al. 2014).

In the Alpine Lateglacial, which spans the time between the decay of the Last Glacial Maximum ice masses [ca. 19–18 ka (Ivy-Ochs 2015)] and the beginning of the Holocene, several Alpine stadials are discussed (Mayr and Heuberger 1968; Winistörfer 1977; Maisch et al. 2003; Kerschner 2009). The last glacier advance of the Late glacial is known as the Egesen stadial, which is linked to the Younger Dryas cold period [Ivy-Ochs et al. (2009) and references therein]. During the Egesen stadial Alpine glaciers advanced several to tens of kilometers down valley and formed multiple moraine ridges recording numerous oscillations at these expanded positions. By 10.0 ka

Editorial handling: G. Milnes.

Electronic supplementary material The online version of this article (https://doi.org/10.1007/s00015-017-0288-x) contains supplementary material, which is available to authorized users.

✉ Olivia Kronig
okronig@phys.ethz.ch

[1] Laboratory of Ion Beam Physics (LIP), ETH Zürich, Otto-Stern-Weg 5, 8093 Zurich, Switzerland

[2] Institute of Geological Sciences, University of Bern, Baltzerstrasse 1+3, 3012 Bern, Switzerland

glaciers were likely smaller than they are today (Solomina et al. 2015). Although several middle Holocene glacier advances have been documented, landforms of this time period are scarce, as their extents were mostly smaller than during the LIA advances of the late Holocene (Patzelt and Bortenschlager 1973; Maisch et al. 1999; Joerin et al. 2006). The glacial landforms of the middle Holocene were either wiped out or overprinted by the more extensive LIA advances, were covered by younger sediments, or they cannot be absolutely dated because there is no material suitable for dating (for example wood or big boulders). This makes a consistent statement about Holocene glacier fluctuations difficult, even in light of abundant research on Alpine glacier reconstructions (Maisch et al. 2003; Ivy-Ochs et al. 2009; Schimmelpfennig et al. 2012, 2014; Hippe et al. 2014). Therefore, it is important to investigate more glacier forefields to improve the overall knowledge about the history of glacier fluctuations in the Alps. The aim of this work was to acquire an overview of different evolutionary stages of the study area during the Holocene, based on detailed field observations combined with cosmogenic nuclide surface exposure and radiocarbon dating. This allowed for chronological reconstruction of the local glacial history based on absolute formation ages of the glacial landforms.

The study area is mentioned in some publications but itself has not been the main topic of research until now. Schneebeli and Röthlisberger (1976) did a study on the different Holocene advances of the Findelgletscher (Findel Glacier) based on its numerous, well-preserved lateral moraines. The left-lateral Findelgletscher moraine was formed during several different advances of the glacier, based on eight paleosols recognized in the moraine by Schneebeli and Röthlisberger (1976). The radiocarbon dating of the four thickest layers showed (uncalibrated) ^{14}C ages between 2565 ± 195 ^{14}C years BP and 845 ± 225 ^{14}C years BP. Further, the study area was part of the diploma and master thesis work of Dick (1991), Coray (2007), Graf (2007) and Madella (2013) in which the forefield of the Findelgletscher, the sedimentology, its moraines and the glacial landforms were investigated.

2 Study site and geomorphic setting

The study area lies in the Valais Alps, east of the village Zermatt (VS) in Switzerland (623972/96968) (Figs. 1, 2). It is located between the north face of a mountain ridge, extending from Gornergrat (3135 m) to the Stockhorn (3532 m) which is oriented west–east, and the 100 m high left-lateral moraine of the Findelgletscher. Today the mountain ridge contains two small glaciers the Triftjegletscher (Triftje Glacier) and one glacier with no name, henceforth called Oberseegletscher (Obersee Glacier). The Triftjegletscher extends from the Hohtälli cable car station (3275 m) to the Stockhorn in the east. The Oberseegletscher is the adjoining glacier of the Triftjegletscher and is in the east connected to the Findelgletscher. Nowadays both glaciers are rather small (0.5–1 km^2) compared to the Findelgletscher (13.08 km^2, 2010) in the north and the Gornergletscher (38.25 km^2, 2003) in the south (WGMS 2015).

The average annual precipitation measured in the study area itself (Station Findeln Haupt 629720/94440, 2680 m) is 666 mm (1958–2010), and based on snow height measurements at the Gornergrat (1992–2011) (626900/92512, 3129 m) a closed snow cover in the study area can be expected from December until June (Based on services of MeteoSwiss). The monthly mean temperatures there range from −9.5 °C in February to 5 °C in August (1993–2013). Since the Gornergrat is approximately 400 m higher, the average temperatures in the study area are expected to be 2–3 °C higher.

Geologically, the study area is located entirely in the Stockhorn unit, a sheared off part of the Mont Fort nappe, a continental subnappe of the Bernhard nappe system (Pleuger et al. 2005). The Mont Fort nappe is made from Variscan gneisses, schists and amphibolites and a post-Variscan cover. The cover contains conglomerates, sandstones, quartzites, marbles, dolomites, marls and flysch (Froitzheim 2001).

The study area can be divided into three subareas as shown in Fig. 3: The Triftjuhöüd in the east, which is mainly the forefield of the small Oberseegletscher, the üsser Höüd the glacier forefield of the Triftjegletscher, and the Findeltriftje or the Verlorenes Tal (lost valley) a bog-like valley formed behind the left-lateral moraine of the Findelgletscher.

3 Methods

Topographic maps, aerial and historic photographs, digital elevation models, geomorphological mapping and surface exposure and radiocarbon dating were combined to reconstruct the local Holocene glacier fluctuations.

3.1 Field work and landform analysis

Detailed geological and geomorphological mapping and interpretation of field relationships built the foundation of the work. A new geomorphological map of the area that was occupied during the Holocene by the Triftje- and the Oberseegletscher resulted (Fig. 4). It also included striation measurements on the glacially polished bedrock, which indicates former ice flow directions. Mapping was supplemented with analysis and implementation of a DEM (Jörg et al. 2012) from LiDAR surveys, which was made

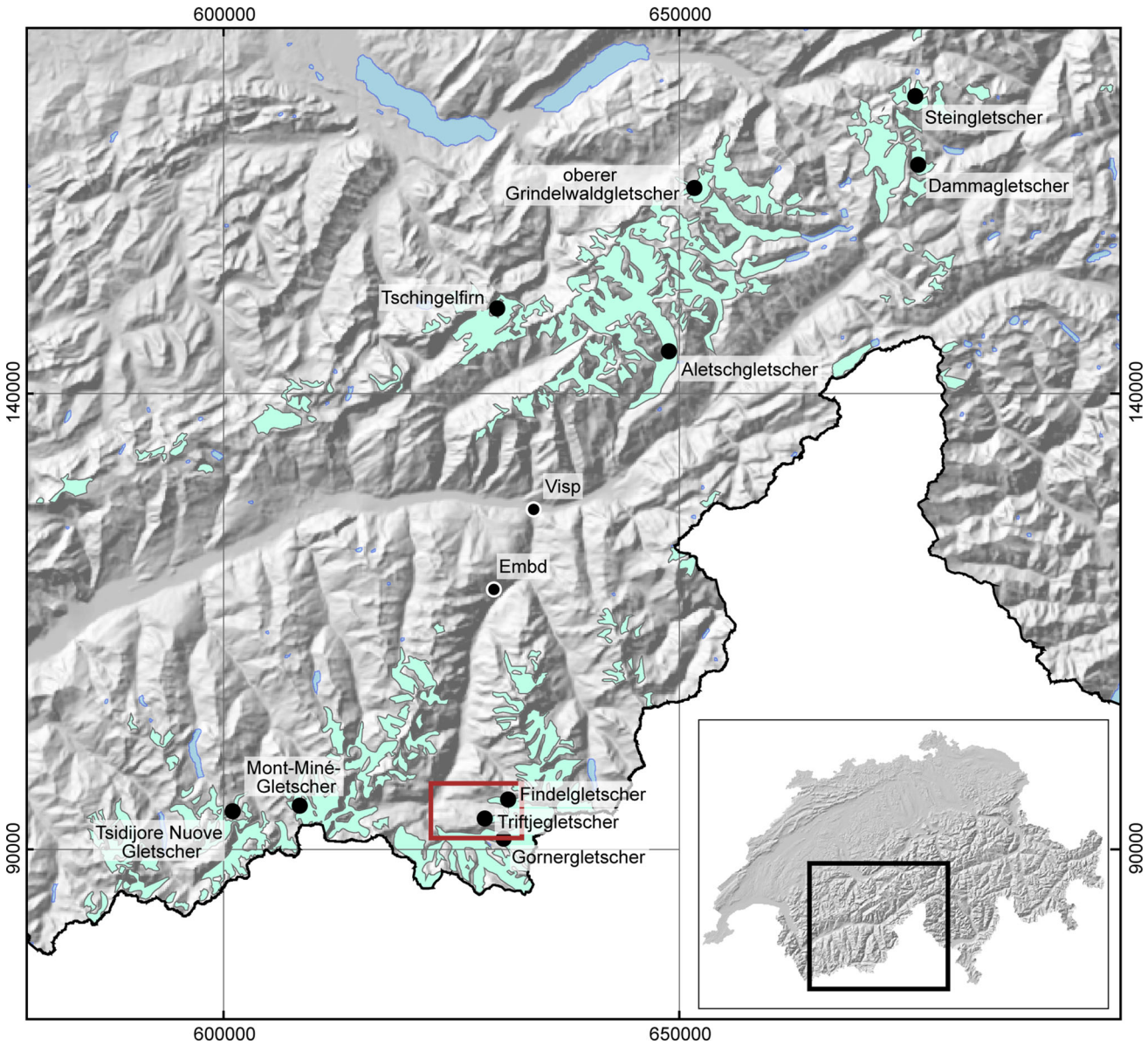

Fig. 1 The hillshade map shows the position of the glaciers mentioned in the text and location of Fig. 2 (red square). The hillshade map is based on the DEM25/200 and glaciers extents are based on the Geological Map of Switzerland 1:500,000 edition 2005 [Reproduced with the authorisation of swisstopo (JA100120)]

available by the Department of Geography of the University of Zurich (GIUZ), and aerial photos [Reproduced with the authorisation of swisstopo (JA100120)] in ArcGIS®. The digital data were a useful tool to decipher the origin of large and discrete landforms that are difficult to see on the ground.

3.2 Exposure dating

Suitable boulders and bedrock samples for exposure dating were carefully chosen based on the field observations and according to the guidelines of Ivy-Ochs and Kober (2008) and Gosse and Phillips (2001). A total of 12 samples (Fig. 3) were collected with hammer and chisel, six boulders on moraine ridges (VT1, VT2, VT7, VT8, VT9, VT12), one boulder of a block deposit in the Triftjuhöüd together with a nearby bedrock sample (VT3, VT4) and two perched boulders also accompanied by nearby bedrock samples (VT5, VT11, VT6, VT10). Most of the samples were concentrated at the outside of the two large moraines, the left-lateral moraine of the Findelgletscher and the right-lateral moraine of the Oberseegletscher, as the landforms there are expected to be pre-LIA in age. Additional samples were taken from the top of the glacially polished bedrock in the üsser Höüd (VT10, VT11) area and one sample at the outermost moraine ridge (VT12) of five small

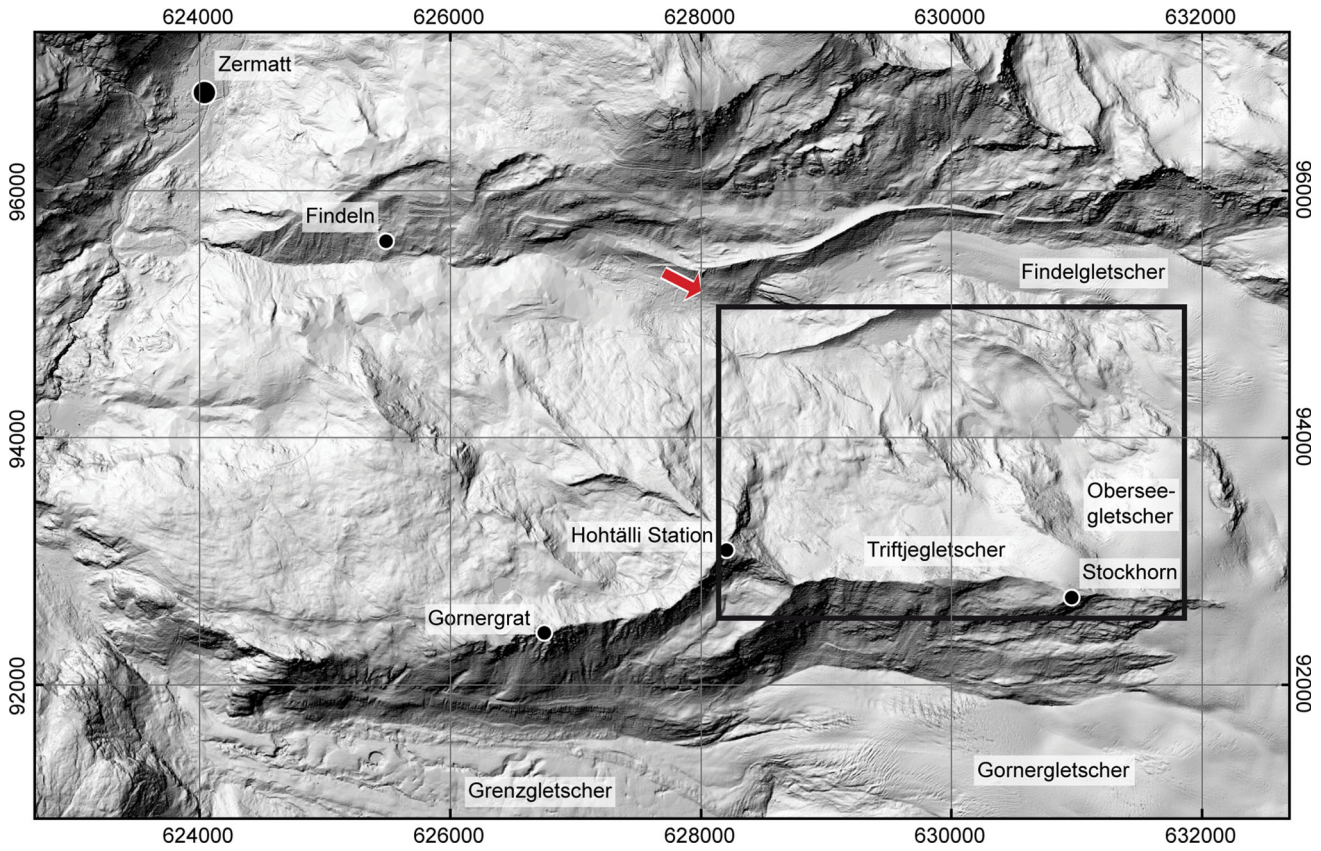

Fig. 2 Overview hillshade map based on the swissALTI3D showing the study area, indicated by the black square (Figs. 4, 5), and the most important mountains, villages and glaciers. The red arrow is showing the view direction of the 2.5 D image of Fig. 3 [Reproduced with the authorisation of swisstopo (JA100120)]

moraines built by the Findelgletscher. The lithology of the samples is gneiss or mica schist, with quartz veins.

The extraction of the ^{10}Be was done after the procedure described in Ivy-Ochs (1996). Where in a first step the samples were crushed and sieved (< 0.8 mm). To isolate the pure quartz, the samples were treated with HF and if the samples were still not pure enough, they underwent an additional separation with a Frantz magnetic separator. 0.25 mg carrier (^{9}Be) was added to the dried quartz and then they were dissolved with supra pure HF (40%). To get rid of unwanted anions and cations the samples were passed through ion exchange resins followed by specific pH precipitation to isolate the Be. ^{10}Be/^{9}Be ratios were measured with the 600 kV Tandy at the ETH Zürich Accelerator Mass Spectrometry (AMS) facility (Christl et al. 2013). The in house standard S2007N, which is calibrated against the 07KNSTD (Nishiizumi et al. 2007) was used.

The surface exposure ages were calculated from the blank corrected (long time laboratory blank of ^{10}Be/^{9}Be = (3.6 ± 2.4) × 10^{-15}) data, using the CRONUS-EARTH online calculator (Balco et al. 2008; 2009) with the northeastern North America ^{10}Be production rate of 3.87 ± 0.19 at/g/a and the scaling model by Lal (1991)/Stone (2000) (scaling scheme 'Lm'). This production rate has been shown to be well applicable to sites in the Alps (Claude et al. 2014) and is in excellent agreement with the recently published global production rates of Heyman (2014) and Borchers et al. (2016). Taking into account for each sample a calculated shielding factor (Balco et al. 2008) as well as an erosion rate of 10^{-4} cm/year (1 mm/k year) and rock density of 2.7 g/cm^3. The given errors are at the 1σ level including analytical uncertainties of the AMS measurements and the blank correction. The exact input data can be found in the Online Resource 1. Besides topographic shielding and sample geometry correction factors, additional snow shielding correction was performed for the three bedrock samples. Therefore, "based on services of MeteoSwiss" a closed snow cover of 124 cm during 7 months was assumed. The snow shielding factor was calculated after Gosse and Phillips (2001), with a snow density of 0.3 g/cm^3 and 109 g/cm^2 for the attenuation length (Zweck et al. 2013; Delunel et al. 2014). The factor was multiplied with the topographic shielding and used as shielding correction input in the CRONUS-EARTH online calculator. Bedrock samples with snow corrected ages are denoted with * in Table 1. We consider the snow

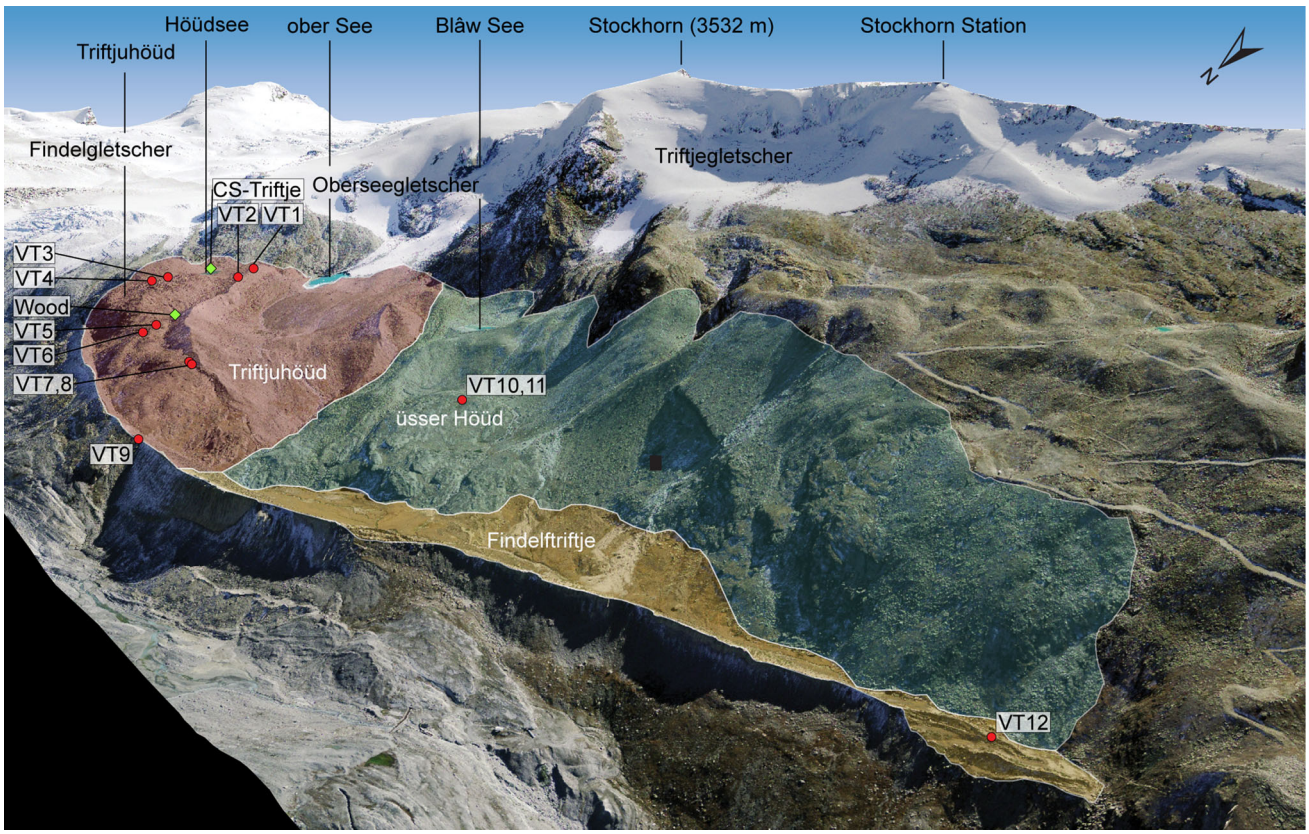

Fig. 3 View of the study area, implemented based on a swissALTI3D (DEM) and SwissImage25, showing the three subareas; shaded in red the Triftjuhöüd, in blue the üsser Höüd and in yellow the Findeltriftje. Red dots show the location of the ^{10}Be and the green squares the location of the radiocarbon samples. As a scale, the left lateral moraine of the Findelgletscher is approximately 2.5 km long. View is to the southeast [Reproduced with the authorisation of swisstopo (JA100120)]

correction as a maximum value, as snow cover during the middle Holocene was likely less (Ivy-Ochs et al. 2009). In the discussion below we implement the ages that have not been corrected for snow cover.

3.3 Radiocarbon dating

During fieldwork, a wood sample, encrusted with till, of approximately 60 cm length and 7 cm diameter was found (630712/94655) sticking out of the lower part of the large right-lateral moraine of the Oberseegletscher (Fig. 3). A fragment was collected to be prepared in the laboratory for radiocarbon dating. The process and the preparation of the sample was done according to Hajdas (2008). Because there was only one sample, it was decided to date it with its extracted cellulose (sample Cellulose 1.1–1.3) and as a control also with different chemical treatments; ABA (sample Wood 1.1–1.3), Soxhlet and ABA (sample Wood 2.1–2.2), Soxhlet and ABOX (sample Wood 3.1–3.2). After the treatments 3.0 mg of the cellulose samples and approximately 2.3–2.5 mg of the wood sample were combusted and graphitized using an elemental analyzer (EA) coupled with a graphitization system "AGE" (Wacker et al. 2010). In this study we include as well the results for a piece of Juniperus found embedded in the lower part of the moraine to the east of the Höüdsee (Fig. 3) by Christian Schlüchter in the early 1990s (sample CS-Triftje). It was dated in 1993 at the Department of Geography at the University of Zurich (GIUZ), and gave a radiocarbon age of 305 ± 70 ^{14}C years BP. Finally, the concentration of ^{14}C/^{12}C was measured with the AMS (Synal et al. 2007). The results of all samples and the CS-Triftje were calibrated using the software OxCal (http://c14.arch.ox.ac.uk) in combination with the IntCal13 atmospheric calibration curve (Reimer et al. 2013). For comparison with ^{10}Be dates, 63 years are added (Table 2) to account for the time between 1950 (BP conventional calibrated radiocarbon time) and 2013 when the sampling was done.

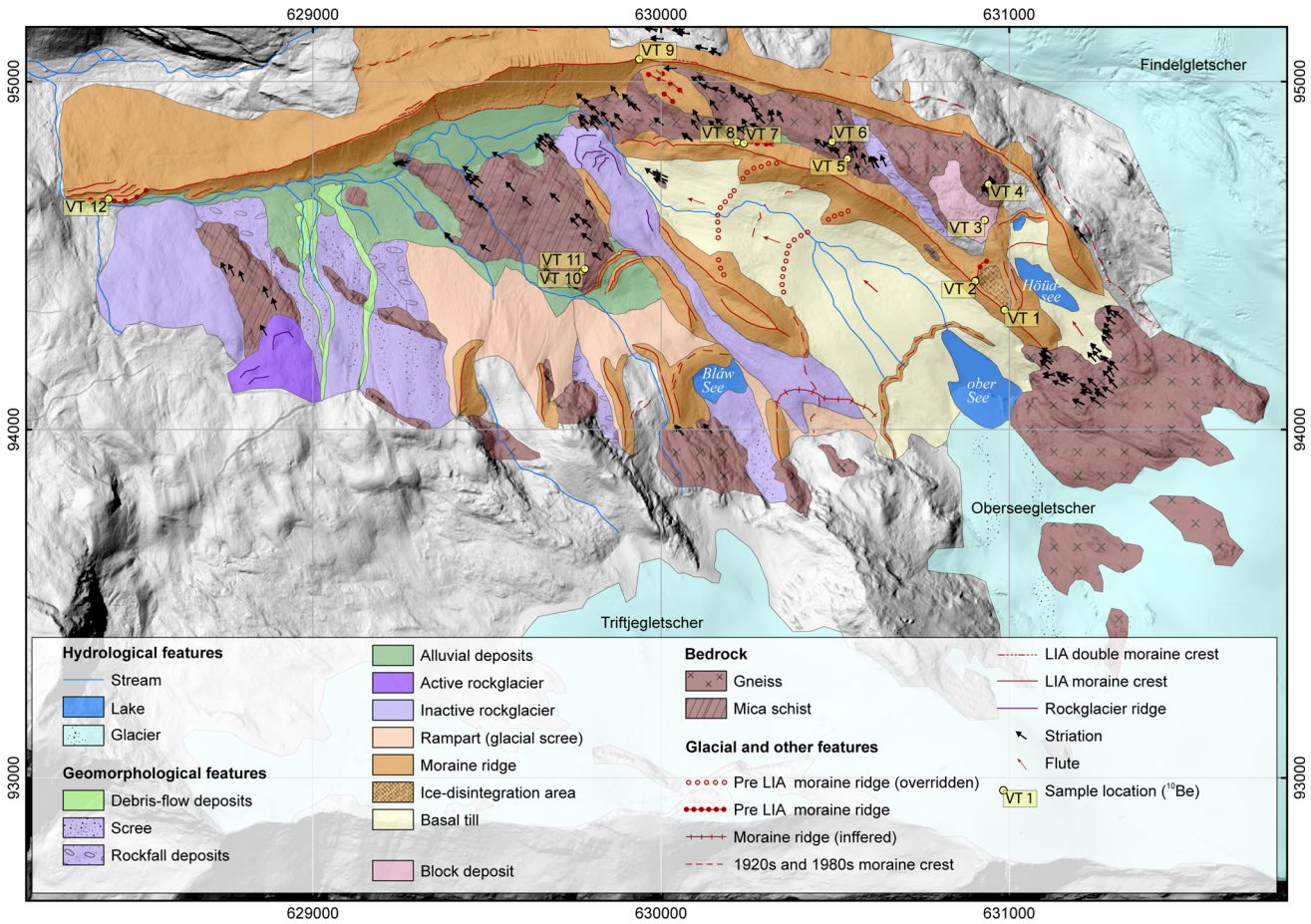

Fig. 4 Map of the study area, with the mapped geomorphological landforms. DEM data used for background hillshade was made available by the Department of Geography of the University of Zurich

4 Results and interpretation

4.1 Geomorphology

The geomorphological map of the study area (Fig. 4) gives a detailed overview of the mapped landforms described in this chapter and the results of striation direction measurements. These were predominately north-west oriented.

The subarea Triftjuhöüd is dominated by the two large lateral moraines (30 m high) of the Oberseegletscher. The Oberseegletscher is still present in the area and ends at a little lake, the ober See. Furthermore the subarea includes a topographic high which reaches an altitude of nearly 2900 m, locally named Triftjuhöüd (Julen and Taugwalder 1995) which gives the subarea its name. Its extent is approximately 2–3 ha and most of it is covered by large angular gneissic boulders (2–7 m) (sample VT3). Dick (1991) mapped this area as “Felsenmeer”, which would imply in situ weathering under periglacial conditions (French 1976). The boulders lie on glacially polished bedrock. Therefore, in this study the landform is mapped as block deposit. Another interesting feature is a crater like landform, which is up to 10 m deep (mapped as ice-disintegration area). It is formed by the right-lateral moraine of the Oberseegletscher, some small moraines next to the Höüdsee and a small moraine perpendicular in between them (sample VT2). An explanation for this crater like structure would be that there was dead ice stored between the moraines left by a former advance of a lobe between the Oberseegletscher and the Findelgletscher.

Between the left-lateral moraine of the Findelgletscher and the right-lateral moraine of the Oberseegletscher there are three approximately 2 m high moraine ridges (630000/95000) on top of the polished bedrock. Because they have a broad and flat shape, a dense vegetation cover and the boulders are covered with an enormous amount of lichens they are mapped as pre-LIA moraines in Fig. 4. They are oriented in a northwest direction, which parallels the orientation of glacial striations in the surrounding bedrock. The moraines were therefore formed during a glacier advance prior to build-up of the huge Findelgletscher left-lateral moraine.

Table 1 Sample informations, AMS measured concentrations of ^{10}Be and calculated surface exposure ages (See also Online Resource 1)

Sample name	Coordinates CH1903/LV03		Altitude (m)	Shielding corr.[a]	^{10}Be[b] × 10^3 (at/g)	Exposure age (year)	Erosion corr. (year)	Snow corr. (year)
VT1	630988	94342	2899	0.9531	14.06 ± 5.54	420 ± 170	420 ± 170	
VT2	630903	94425	2881	0.9931	44.21 ± 5.61	1270 ± 160	1270 ± 160	
VT3	630930	94600	2884	0.9943	106.12 ± 6.78	3050 ± 200	3050 ± 200	
VT4[c]	630941	94704	2883	0.9936	410.42 ± 17.56	11,720 ± 500	11840 ± 510	14240 ± 620
VT5	630537	94777	2812	0.9946	376.53 ± 15.72	11,330 ± 470	11430 ± 480	
VT6[c]	630492	94826	2804	0.9946	405.16 ± 11.04	12,460 ± 340	12590 ± 350	15140 ± 420
VT7	630239	94821	2765	0.9921	51.15 ± 8.39	1590 ± 260	1590 ± 260	
VT8	630220	94825	2761	0.9935	34.47 ± 7.94	1060 ± 240	1060 ± 250	
VT10[c]	629777	94455	2702	0.9827	314.08 ± 13.02	10170 ± 420	10250 ± 430	12330 ± 790
VT11	629777	94455	2702	0.9830	351.24 ± 11.75	11230 ± 380	11330 ± 380	
VT12	628416	94661	2511	0.9844	25.61 ± 3.32	970 ± 130	970 ± 130	

Sampling and measurement was done in 2013. Snow corrected ages are shown for comparison. Erosion corrected ages are used in the discussion

[a] Shielding correction includes the topographic shielding due to surrounding landscape and the dip of the sampled surface. Additionally for the bedrock samples a snow shielding correction factor of 0.8313 was multiplied with the shielding correction (see text)

[b] AMS measurement errors are at the 1σ level

[c] Bedrock samples. All others are from boulders

Table 2 Radiocarbon ages obtained on wood sample of this study, the CS-Triftje sample and the radiocarbon ages from Schneebeli and Röthlisberger (1976)

Sample	Altitude (m)	ETH- Code	Material	Treatment	^{14}C Age (yr BP)	Error (yr)	cal ^{14}C Age (cal yr BP)	cal ^{14}C Age before 2013 (cal yr before 2013)
This study								
Cellulose 1.1		ETH-54927	cellulose	ABA, Cellulose	203	27		
Cellulose 1.2		ETH-54927	cellulose	ABA, Cellulose	185	23	293 - 0	356 - 63
Cellulose 1.3		ETH-54927	cellulose	ABA, Cellulose	176	23		
Wood 1.1		ETH-54926	wood	ABA	113	26		
Wood 1.2		ETH-54926	wood	ABA	98	23	266 - 17	329 - 80
Wood 1.3		ETH-54926	wood	ABA	118	23		
Wood 2.1		ETH-54926	wood	Soxhlet, ABA	158	34	296 - 0	359 - 63
Wood 2.2		ETH-54926	wood	Soxhlet, ABA	198	34		
Wood 3.1		ETH-54926	wood	Soxhlet, ABOX	150	34	291 - 0	354 - 63
Wood 3.2		ETH-54926	wood	Soxhlet, ABOX	173	34		
Schlüchter 1993								
CS-Triftje		UZ-1544	wood		305	70	508 - 0	571 - 63
Schneebeli and Röthlisberger 1976								
HV-6791	2560		paleosol		845	225	1277 - 495	1340 - 558
HV-6792	2560		paleosol		1025	225	1364 - 557	1427 - 620
HV-6793	2525		paleosol		1610	115	1805 - 1300	1868 - 1363
HV-6794	2020		paleosol		2565	195	3156 - 2155	3219 - 2218

At the distal side of the right-lateral moraine of the Oberseegletscher there are two small moraine ridges (1 m) that are much smaller and just slightly external to the large right-lateral moraine (VT7, VT8). Their formation is not completely clear, but they are older than the large right-lateral moraine which overtops and nearly completely buries them (indicated by pre-LIA moraine ridge in Fig. 4). This indicates more extensive advances of the Oberseegletscher before the construction of the large LIA moraines. More evidence is given by two spurs that can be observed extending inwards from both lateral moraines of the Oberseegletscher. These landforms can be followed as soft hills throughout the basal till that extends across to the other lateral moraine. They are interpreted as moraines formed during older stadials, which were overrun by a next, larger advance. It is exceptional that they are still nicely visible, especially on the hillshade map and on aerial photos. The borders of the Triftjuhöud subarea consist to the east and north of the prominent left-lateral moraine of the Findelgletscher, and to the west, of a strongly elongated landform (1 km long and 40–140 m wide), that crosscuts the area from southeast to northwest. At its tongue it has a well-defined margin and shows also furrow and ridge morphology. Further flow lines can be followed from the onset almost to the end of the landform, those are all typical indicators for a rockglacier (Barsch 1996).

In the subarea üsser Höüd the Triftjegletscher has retreated to higher areas and is not present in the study area itself anymore. In the steep slope in the front of the glacier gneissic bedrock is outcropping. Below the bedrock two large moraine ramparts (> 80 m high) formed (Fig. 4). To the west scree and rockfall material were deposited, which is in part incised by debris-flow channels. On the mountainside there is almost no vegetation as the scree is unstable. At the western end an inactive and an active rockglacier can be found. In the east a lake called Blâw See exists, rimmed by a small moraine ridge and two more moraines (1–3 m) at the foot of the rampart. They are the most distal and therefore oldest moraines left by the Triftjegletscher in its proglacial area. From there on, there are extensive outcrops of glacially polished mica schist (VT10 and VT11) which end with a rather steep bedrock step.

This step builds the transition to the third subarea, the Findeltriftje, a narrow bog-like valley that formed behind the large left-lateral moraine of the Findelgletscher and the mountain slope. At its western end, which is marked by a bedrock knob, there are five small (1–5 m) parallel moraine ridges (sample VT12) (also shown as pre-LIA moraine ridge on Fig. 4). They provide clear evidence for several advances of the Findelgletscher, since they were truncated during advances when the large lateral moraine was formed; they have to be older.

4.2 Exposure dating

Detailed sample information and results of the cosmogenic nuclide dating are shown in Table 1 and Fig. 5. The obtained exposure ages range from 420 ± 170 a (VT1) to 12590 ± 350 a (VT6). The ages can be grouped into three different age ranges. A first group contains the ages of the late Lateglacial to early Holocene. This includes all the bedrock samples (VT4, VT6, VT10) and the two corresponding perched boulder samples (VT5, VT11). In the second group are ages around 1200 a, those are all boulders on moraines (VT2, VT7, VT8, VT12). In the last, third group is only one sample (VT1) which has been exposed for 420 ± 170 a. The only sample that does not fit into one of these groups is sample VT3 with 3050 ± 200 a, the boulder in the block deposit. Sample VT9 was lost during sample preparation.

4.3 Radiocarbon dating

An overview of the applied treatments of the wooden sample, the results of the radiocarbon dating and the calibrated ages from the wood sample CS-Triftje and from Schneebeli and Röthlisberger (1976) are summarized in Table 2 and Fig. 5. The uncalibrated and also the calibrated ages of the samples with the ABA treatment (Wood 1.1–1.3) show substantial younger ages of 266–17 cal - years BP (329–80 cal years before 2013) compared to the samples prepared with other treatments, which have a more consistent age range. The average radiocarbon age of the cellulose treatment is 293–0 cal years BP (356–63 cal - years before 2013). The variance between the ages originates most likely from the wood itself. The wood had a very twisted growth habit, which results in some parts having numerous growth rings in the space of a few millimeters. Furthermore, the radiocarbon age determination of the wood sample intersects the calibration curve at a radiocarbon plateau. This results in a complicated probability distribution and is responsible for the broad range of the calibrated ages.

The calibrated age of CS-Triftje gave an age range of 508 cal years BP to modern (571–63 cal years before 2013). Consulting a historic photograph from 1949 (ETH-Bibliothek Zürich, Bildarchiv, https://doi.org/10.3932/ethz-a-000018701), shows that the location was covered by the glacier at that time. This allows to limit the age from 508–1 cal years BP (571–64 cal years before 2013).

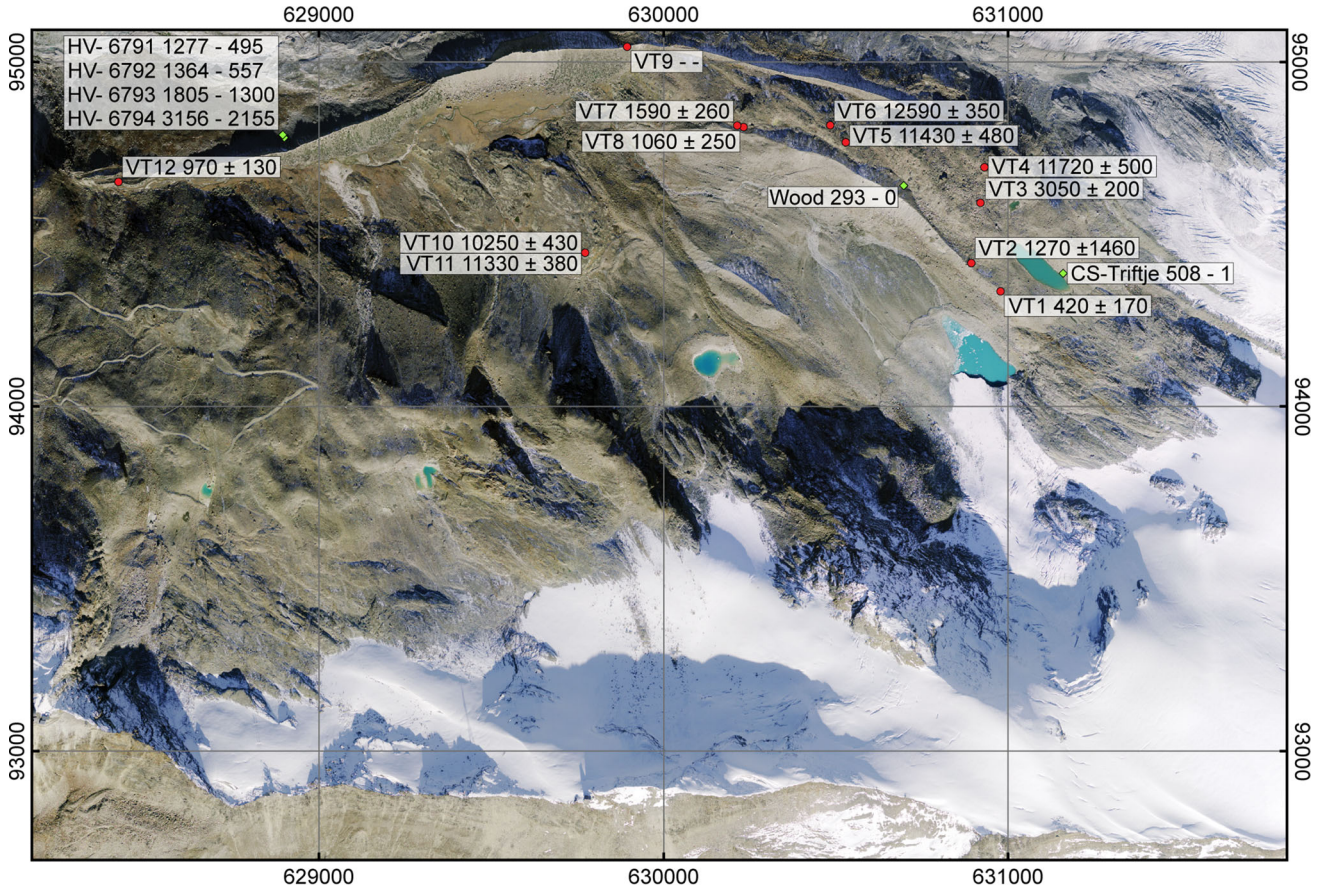

Fig. 5 SwissImage25 of the study area, showing the sample locations (red dots) and the exposure ages (in years). The location (green squares) and the radiocarbon age of the wood sample, the CS-Triftje sample and the recalibrated ages dated by Schneebeli and Röthlisberger (1976) are given in cal years BP [Reproduced with the authorisation of swisstopo (JA100120)]

5 Chronology of glacier advances in the study area

Based on crosscutting relationships observed in the field, three different stadials were distinguished; pre-LIA, LIA and post-LIA. The obtained radiocarbon and the exposure ages complement and underpin the field observations. As elucidated in Sect. 4.1, the direction of the three pre-LIA moraines (630000/95000) and striations measurements on the glacially polished bedrock outcropping adjacent to the Findletriftje and close to the large left-lateral moraine of the Findelgletscher offer the following important evidence that the bedrock record the oldest advances. This is supported by the exposure age of the polished surfaces (VT4, VT6, VT10). Those ages (11720 ± 500 a, 12460 ± 340 a, 10170 ± 420 a) dating to the early Holocene describe the decay of the Egesen stadial glaciers (Fig. 6). Note, that the snow-corrected ages for the bedrock (Table 1) are distinctly older than the corresponding ages of the perched boulders (VT5: 11330 ± 470 a and VT11: 11330 ± 380 a). The most reasonable explanation is a too high assumption for the snow cover. Applying modern weather data values to the entire Holocene has a large uncertainty. But it gives a rough idea of how big the influence of snow amount and duration might be. Further, if the uncorrected ages of the bedrock and the corresponding perched boulder are compared one should expect, that the age of the bedrock should be younger due to additional shielding by the snow cover. Because it is assumed, that snow accumulates more easily on bedrock than on a boulder, where wind and other factors have a stronger influence on the amount of snow that will be accumulated. This should lead to an age underestimation of the bedrock sample. This is true for bedrock-boulder pair VT10/VT11 but not for VT6/VT5, where the exposure age of the bedrock sample is older. One possibility is that in this location abrasion of the glacier may not have been sufficient to remove all the ^{10}Be from pre-exposure and the age of VT6 is slightly overestimated (Wirsig et al. 2017).

Several boulders that lie outside of the LIA extent were dated (VT2, VT7, VT8, VT12). The oldest sample of this group is VT7, which yielded an age of 1590 ± 260 a. It is

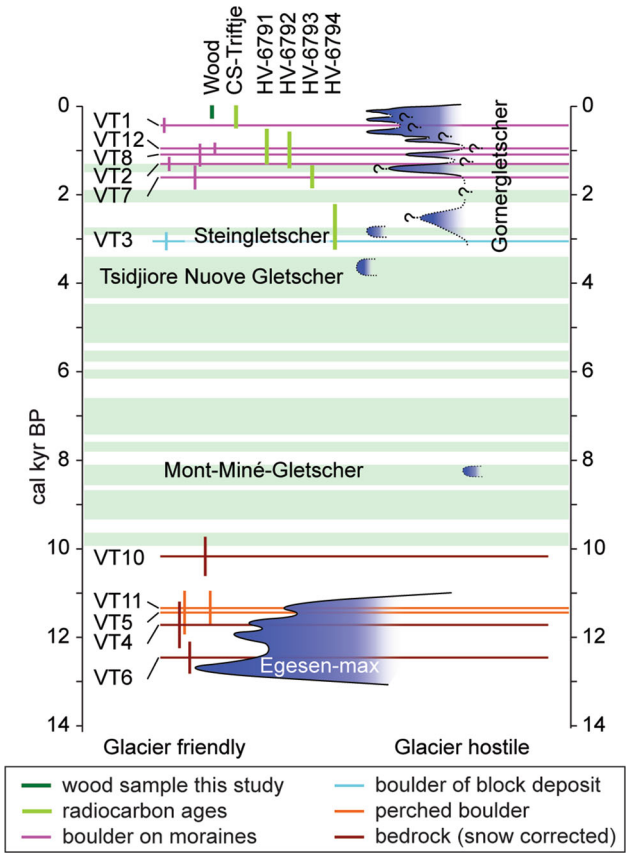

Fig. 6 Exposure and radiocarbon ages of this study and radiocarbon ages of Schneebeli and Röthlisberger (1976) in comparison with a summary of glacier variations during the Lateglacial and the Holocene, modified after Ivy-Ochs et al. (2009). Glacier advances are shown as blue curves. Green bars show 12 periods of glacier recession (Joerin et al. 2006). LIA fluctuation of the Gornergletscher are based on Holzhauser et al. (2005). Advances of Steingletscher, Tsidjiore Nuove Gletscher after Schimmelpfennig et al. (2012, 2014) and Mont-Miné-Gletscher after Nicolussi and Schlüchter (2012)

one of the two samples taken on the small moraine ridge that is cross cut and partially buried by the large lateral LIA moraine of the Oberseegletscher (Figs. 3, 4). The second sample (VT8), taken at the same small moraine ridge, gave a younger age of 1060 ± 250 a. Both samples however have almost overlapping errors. Based on their proximity we may relate the timing of formation of the two overrun moraines that were recognized in the field and on the hillshade map (Fig. 4). If the more distal overrun moraine ridge of the Oberseegletscher belongs to the same advance when the small dated moraines were formed (VT7, VT8), then the second, proximal, overrun moraine ridge was formed during a subsequent stagnation period prior to the LIA re-advance. Conversely, perhaps it was formed by a small advance, eventually during the early LIA. The youngest sample of this early late Holocene group is VT12 (970 ± 130 a). This boulder is located on the outer-most moraine in a series of stacked moraines of the Findelgletscher left-lateral moraine (Figs. 3, 4). Within the stated errors, it may be concluded that the Findelgletscher advanced at a similar time as the Oberseegletscher, with perhaps a delayed response reflecting its greater volume. The ages and field observations suggest that the glaciers in the study area, reached about the size of their LIA extent during this cold interval, around 1200 years ago.

Our exposure age of 420 ± 170 a (VT1) from the right-lateral moraine of the Oberseegletscher agrees well with the LIA as shown on the Dufour map (Dufour 1862). This is true as well for the radiocarbon age (356–63 cal years before 2013) of the piece of wood found embedded in this same moraine. The radiocarbon age of the CS-Triftje wood with 571–63 cal years before 2013 suggests that the Juniperus was overrun by an early LIA advance and that the location was covered by the glacier at least during the last LIA advance, perhaps until 1949 (ETH-Bibliothek Zürich, Bildarchiv, https://doi.org/10.3932/ethz-a-000018701).

A special case is sample VT3, the boulder of the block deposit. The exposure age gives for its deposition a minimum age of 3050 ± 200 a. Combined with the field observation that the blocks are lying on glacially polished bedrock which was dated to 11840 ± 510 a (VT4), the block deposit may have formed sometime during the middle Holocene.

The calibrated radiocarbon ages originally dated by Schneebeli and Röthlisberger (1976) give detailed insight into to the Findelgletscher fluctuations during the Holocene. They dated four paleosol layers that outcropped along the inside of the left-lateral moraine of the Findelgletscher. Each paleosol layer testifies to a relatively long, glacier-hostile period. Due to collapse of the moraine ridge, the soil layers are no longer exposed today. The lowest exposed and dated soil (HV-6794) in the study of Schneebeli and Röthlisberger (1976) developed on a lateral moraine. Thus it can be concluded, that there was already a glacier advance before the paleosol was formed. The calibrated radiocarbon age of this first paleosol (HV-6794) has an age range of 3156–2155 cal years BP (3219–2218 cal years before 2013), which can be roughly correlated with the subsequent glacier advance that deposited the next till layer on the top of the paleosol (Schneebeli and Röthlisberger 1976). In the stratigraphic profile there are two additional, small paleosols before the next prominent, dated one. This suggests that there were several advances, or fluctuations of the glacier. Then most likely a long warmer period followed which allowed the next thick paleosol to form. The age range of this paleosol (HV-6793) is 1805–1300 cal years BP (1868–1363 years before 2013). The subsequent advance that can be linked to this age, which was shortly interrupted by a warm period

that left a minor paleosol layer, deposited approximately 20 m of homogeneous till and therefore can be interpreted as a single glacier advance. The soil dated with HV-6792 is on top of the large till deposit and has an age of 1364–557 cal years BP. It is buried under a thin till layer, followed by the next thin paleosol, which was not dated. The last paleosol only 0.5 m below the moraine crest of 1976, has an age 1277–495 (HV-6791). These radiocarbon ages show, that soil was buried at 3.2–2.2, 1.8–1.3, 1.4–0.6, 1.3–0.5 cal ka BP. Therefore, there were several advances or fluctuations of the Findelgletscher at expanded positions before the LIA (Schneebeli and Röthlisberger 1976).

6 Comparison with late Lateglacial to Holocene chronological framework in the Alps

6.1 Lateglacial

Moraines of the Findelgletscher attributed to the Egesen stadial can be found on both sides of the mountain flanks (Winistörfer 1977). On the right side of the Findelgletscher there are several moraine ridges that can be followed until a little above the village of Findeln (Fig. 2). It is assumed that Winistörfer (1977) assigned these moraines to the Egesen stadial. He estimated the glacier terminus at that time was close to Embd. Unfortunately the Egesen glacier extent drawn by Winistörfer (1977) is not distinct around the Triftjegletscher. However, according to the elevation of the preserved moraines, it is likely, that during the Egesen stadial the study area was completely covered by ice. The oldest ^{10}Be exposure ages (VT4, VT5, VT6, VT10, VT11) and the north-northwest direction of the striations on the bedrock between the left-lateral moraine of the Findelgletscher and the right-lateral moraine of the Oberseegletscher support this interpretation. Also the three moraine ridges on this polished bedrock (630000/95000) likely formed at the end of this phase. Therefore, it can be concluded that the area was covered by a combined Triftje-, Obersee-, and Findelgletscher until approximately 12,000–11,000 years ago, when the first bedrock islands were appearing. This coincides with the timing of downwasting of the Egesen stadial of the Grosser Aletschgletscher (Kelly et al. 2004), Steingletscher (Schimmelpfennig et al. 2014) and at several other sites in the Alps (Ivy-Ochs et al. 2009; Moran et al. 2016; Baroni et al. 2017).

6.2 Holocene and Little Ice Age

Based on the observations and the ^{10}Be data the glaciers in the study area were in a recessional phase in the early to middle Holocene (Fig. 6). Either there were no landforms built during this time or those that were built, were destroyed by younger and more extensive advances. It is likely that all across the Alps glaciers were smaller than their LIA extents during the early and middle Holocene as shown by radiocarbon data from wood and peat washing out of the presently melting glaciers (Hormes et al. 2001; Joerin et al. 2006; Nicolussi and Schlüchter 2012). This overlaps with the Holocene Thermal Maximum discussed as an at least northern Hemisphere if not global phenomena which lasted from about 9 to 5 ka (Renssen et al. 2009; Seppä et al. 2009; Charpentier Ljungqvist 2011).

In Greenland ice core data, a climatic cooling at 8.2 ka has been recognized (Alley et al. 1997). The effect of this cold period also was documented in the Alps with isotope records from lake sediments (von Grafenstein et al. 1998, 1999) and speleothems (Boch et al. 2009). Nicolussi and Schlüchter (2012) found the first direct evidence of glacier activity related to this cooling at Mont-Miné-Gletscher, based on dendrochronological analyses of tree remnants and trunks they collected in the outwash plain. Nevertheless, the glacier extent was significantly smaller than it was during the LIA. No indications for a glacier advance at 8.2 ka were found in this study. Recent studies for example at Tsidjiore Nuove Gletscher (Schimmelpfennig et al. 2012) found as well no evidence for glacial activity during the middle Holocene.

Several sites in the Alps (Fig. 1) have evidence of multiple advances during the Löbben Period (ca. 3800–3400 a) which was first described by Patzelt and Bortenschlager (1973) and Patzelt (1977). Evidence has been found for example, at the Gornergletscher and the Grosser Aletschgletscher by Holzhauser (1995), at Steingletscher (Schimmelpfennig et al. 2014) and at the Tschingelfirn where four ridges were assigned to this cold period (Wipf 2001). Although no landforms of this time were found in the mapped study area, the lowest ^{14}C dated buried soil [HV-6794: 3156–2155 cal years BP (3219–2218 cal years before 2013)], did form on glacial sediment of the Findelgletscher left-lateral moraine. Thus, the glacier advance prior to soil formation may correspond to the Löbben oscillation. On the other hand, the till that buried this soil indicates an advance of the Findelgletscher sometime after 3219–2218 cal years before 2013 (Schneebeli and Röthlisberger 1976), which roughly would correspond to the Göschenen I stadial (3000–2300 a) (Zoller et al. 1966; Burga et al. 2001). New ^{10}Be data show that Steingletscher (Fig. 2) advanced to a position slightly more extensive than the LIA, around this time as well (Schimmelpfennig et al. 2014). The Göschenen I stadial may correspond to the 2.8 ka event documented in several climate studies (Swindles et al. 2007; Wang et al. 2013) and dated glacier advances in North America (Menounos et al. 2009; Wiles et al. 2011).

In the study area distinct evidence for at least one advance during the Göschenen II cold phase [1600–1200 a (Zoller et al. 1966)] is provided by dates from boulders on the small moraine ridges that lie just outside the large right-lateral moraine of the Oberseegletscher (VT7 1590 ± 260 a, VT8 1060 ± 250 a) (Fig. 5). The overrun frontal moraine in the Oberseegletscher forefield may also have formed in this time period. This result confirms observations from the Dammagletscher where this stadial—Göschenen II—was first described by Zoller et al. (1966). Most recently also at Mer de Glace an advance during the Göschenen II is shown by several radiocarbon- and dendrochronologically dated wood samples, found embedded in the moraine (Le Roy et al. 2015). The timing of these glacier advances coincides with the "Dark Ages Cold Period" and "Late Antique Little Ice Age" climate event(s) noted at numerous Northern Hemisphere sites (Büntgen et al. 2016; Helama et al. 2017). Furthermore, the boulder (VT2) of the crater like landform (indicated as ice disintegration area in Fig. 4) with an age of 1270 ± 160 a suggest as well an affinity with a cold phase during the Göschenen II period. It shows that there was a remnant ice block at this position between the bedrock to the northeast and the right-lateral moraine of the Oberseegletscher to the southwest. The outer-most, of the stacked Findelgletscher left-lateral moraines has an age of 970 ± 130 a (VT12). The advance when this moraine formed may correspond to one of the two advances where the paleosols were buried (HV-6792: 1427–620 cal years before 2014, HV-6791: 1340–558 cal years before 2013) (Schneebeli and Röthlisberger 1976). Those field observations suggest that, in the study area this advance, which we relate to the Göschenen II period, had about the same the extent as the LIA.

During the LIA, which started around 600 years and lasted until 100 years ago (Lüthi 2014; Le Roy et al. 2015; Solomina et al. 2015), glacier advances built most of the landforms that shape the glacier forefields in the Alps nowadays. Among others Holzhauser (2010) recognized three significant glacier advances during the LIA at Gornergletscher and at Grosser Aletschgletscher. Further, Zumbühl (1980) describes an advance of the Grindelwaldgletscher around 1246/47AD (ca. 700 a). A second LIA advance is documented at Gornergletscher, Grosser Aletschgletscher and also Grindelwaldgletscher and reached a maximum around 1350 AD (ca. 600 a) (Holzhauser et al. 2005). Those advances were followed by the most extensive advance of Alpine glaciers in 1850/60 as documented in Switzerland on the Dufour maps (Dufour 1862). At our study site, this is shown by one exposure age of the Oberseegletscher LIA moraine (VT1) with 420 ± 170 a and the radiocarbon age of the wood sample 293–0 cal years BP (356–63 cal years before 2013) found embedded in the same moraine.

6.3 Recent glacier extents and future prospective

The youngest landforms of the study area are the small moraine ridges (0.5–2 m) from the 1920s and the 1980s advances that rim the Blâw See and the ober See. They were mapped based on field observations, official topographic maps [Reproduced with the authorisation of swisstopo (JA100120)], aerial photos and the glacier monitoring data by the Versuchsanstalt für Wasserbau (VAW) (Glaciological reports 1881–2017). The length change measurements at the Findelgletscher show it advancing until 1894 before it continuously started to retreat 4–16 m a year (Rastner et al. 2016). This was interrupted by an advance of 52 m between 1916 and 1920. After this intermezzo, the glacier was retreating until 1979 with a maximum length change of − 478 m in the year 1957/58. The general retreating was interrupted again from 1979 to 1985 by a readvance of 246 m. Since then the glacier retreats between 18 and 358 m per year. In total the Findelgletscher lost 2496 m in length from 1885 to 2015 (Glaciological reports 1881–2017). According to mass balance models, the Triftje and the Oberseegletscher are now at an elevation where they are in balance or even show a positive mass balance (Paul et al. 2008). In the future, ongoing retreat of the glaciers in the study area is expected, the same as for most of the glaciers in the Alps (Haeberli and Hohmann 2008).

7 Conclusions

Based on detailed field work combined with ^{10}Be exposure and radiocarbon dating, we reconstructed the history of glacier fluctuations of the Triftje- and the Oberseegletscher over the last ca. 12,000 years. Consistent northwest orientation of glacial striations suggests that a coalesced Triftje-, Obersee- and Findelgletscher completely covered the study area during the Egesen stadial at the end of the Pleistocene. As the Egesen glaciers separated and retreated, the bedrock became successively ice-free between 12590 ± 350 a and 10250 ± 430 a based on ^{10}Be results. Landforms attributable to the middle Holocene were neither observed nor dated in the study area. This is in agreement with other study sites in the Alps, where landforms of this time period are rare. Previously published radiocarbon dates point to an advance of the Findelgletscher in the early part of the late Holocene as the lower part of the 100 m-high left-lateral moraine was deposited. Further buried paleosols in this moraine document subsequent advances at 3.2–2.2, 1.8–1.3, 1.4–0.6, 1.3–0.5 cal ka

BP. As shown by the boulder ^{10}Be date (VT12: 970 ± 130 a), the outer-most of the five, stacked lateral moraines along the left-hand side of the Findelgletscher was constructed during the advance in which one of the upper soils was buried. Three ^{10}Be dates on moraine boulders of the Oberseegletscher (VT2, VT7, VT8), which range from 1590 ± 260 a to 1060 ± 250 a show, it as well advanced at the same time. Those four ^{10}Be dates and radiocarbon data clearly document advances of the Oberseegletscher and the Findelgletscher during the Göschenen II stadial, contemporaneous with the Dark Ages Cold Period. During the LIA, glaciers in the study area re-advanced; the Oberseegletscher constructed 65 m-high lateral moraines. In these advances most of the already existing landforms were destroyed, except in the forefield of the Oberseegletscher where two overrun moraine ridges can still be recognized. Age data from the right-lateral Oberseegletscher moraine (VT1: 420 ± 170 a and wood sample: 356–63 years before 2013) testify to formation of much of the moraine during the LIA, as shown on topographic maps of that time. Although the largest moraines in the glacier forefields are called 'Little Ice Age' moraines, they are often actually composite moraines that built-up during numerous late Holocene advances. We tracked post-LIA glacier variations based on aerial photos and available topographic maps. Through the combination of comprehensive field mapping with isotopic dating we have sharpened the focus on late Holocene glacier variations. Evidence for glacier advances during the Dark Ages Cold Period is especially compelling.

Acknowledgements Two anonymous reviewers are thanked for their constructive criticisms. We would like to thank the GIUZ and the VAW for making the high resolution DEM and aerial photos available. The meteorological data was provided by MeteoSwiss, the Swiss Federal Office of Meteorology and Climatology. A special thanks to the Laboratory of Ion Beam Physics ETHZ group for their excellent AMS measurements. Further, we are deeply grateful for the support from Bergbahnen and the Burgergemeinde of Zermatt. We would also like to thank CH-Quat for their financial support for fieldwork. This research was partially supported by SNF Grant 135448.

References

Alley, R. B., Mayewski, P. A., Sowers, T., Stuiver, M., Taylor, K. C., & Clark, P. U. (1997). Holocene climatic instability: A prominent, widespread event 8200 yr ago. *Geology, 25,* 483–486.

Balco, G., Briner, J., Finkel, R. C., Rayburn, J. A., Ridge, J. C., & Schaefer, J. M. (2009). Regional beryllium-10 production rate calibration for late-glacial northeastern North America. *Quaternary Geochronology, 4,* 93–107.

Balco, G., Stone, J. O., Lifton, N. A., & Dunai, T. J. (2008). A complete and easily accessible means of calculating surface exposure ages or erosion rates from ^{10}Be and ^{26}Al measurements. *Quaternary Geochronology, 3,* 174–195.

Baroni, C., Casale, S., Salvatore, M. C., Ivy-Ochs, S., Christl, M., Carturan, L., et al. (2017). Double response of glaciers in the Upper Peio Valley (Rhaetian Alps, Italy) to the Younger Dryas climatic deterioration. *Boreas, 46,* 783–798.

Barsch, D. (1996). *Rockglaciers: indicators for the present and former geoecology in high mountain environments* (p. 331). Berlin: Springer.

Boch, R., Spotl, C., & Kramers, J. (2009). High-resolution isotope records of early Holocene rapid climate change from two coeval stalagmites of Katerloch Cave, Austria. *Quaternary Science Reviews, 28,* 2527–2538.

Böhlert, R., Egli, M., Maisch, M., Brandova, D., Ivy-Ochs, S., Kubik, P. W., et al. (2011). Application of a combination of dating techniques to reconstruct the Lateglacial and early Holocene landscape history of the Albula region (eastern Switzerland). *Geomorphology, 127,* 1–13.

Borchers, B., Marrero, S., Balco, G., Caffee, M., Goehring, B., Lifton, N., et al. (2016). Geological calibration of spallation production rates in the CRONUS-Earth project. *Quaternary Geochronology, 31,* 188–198.

Büntgen, U., Myglan, V. S., Ljungqvist, F. C., McCormick, M., Di Cosmo, N., Sigl, M., et al. (2016). Cooling and societal change during the Late Antique Little Ice Age from 536 to around 660 AD. *Nature Geoscience, 9,* 231–236.

Burga, C. A., Perret, R., & Zoller, H. (2001). Swiss localities of early recognized Holocene climate oscillations: Characterization and significance. *Vierteljahrsschrift der Naturforschenden Gesellschaft in Zürich, 146,* 65–74.

Charpentier Ljungqvist, F. (2011). The spatio-temporal pattern of the mid-Holocene thermal maximum. *Geografie-Sborník ČGS, 116,* 91–110.

Christl, M., Vockenhuber, C., Kubik, P. W., Wacker, L., Lachner, J., Alfimov, V., et al. (2013). The ETH Zurich AMS facilities: Performance parameters and reference materials. *Nuclear Instruments & Methods in Physics Research Section B-Beam Interactions with Materials and Atoms, 294,* 29–38.

Claude, A., Ivy-Ochs, S., Kober, F., Antognini, M., Salcher, B., & Kubik, P. W. (2014). The Chironico landslide (Valle Leventina, southern Swiss Alps): age and evolution. *Swiss Journal of Geosciences, 107,* 273–291.

Coray, S. (2007). *Glazialsedimentologische Untersuchungen an Flutes im Vorfeld des Findelengletschers. Master Thesis*, Universität Bern, unpublished, 116 pp.

Deline, P., & Orombelli, G. (2005). Glacier fluctuations in the western Alps during the Neoglacial, as indicated by the Miage morainic amphitheatre (Mont Blanc massif, Italy). *Boreas, 34,* 456–467.

Delunel, R., Bourles, D. L., van der Beek, P. A., Schlunegger, F., Leya, I., Masarik, J., et al. (2014). Snow shielding factors for cosmogenic nuclide dating inferred from long-term neutron detector monitoring. *Quaternary Geochronology, 24,* 16–26.

Dick, K. (1991). *Geologische Kartierung Fluhalp -Verlorenes Tal (Findelengletscher) bei Zermatt/VS Teil A* (p. 16). Zürich: Diplomarbeit, ETH Zürich.

Dufour, G.-H. (1862). *Topographische Karte der Schweiz, Blatt XXIII: Domo d'Ossola*. Arona: Eidgenössische Landesopographie Schweiz.

French, H. M. (1976). *The periglacial environment* (p. 309). London: Longman.

Froitzheim, N. (2001). Origin of the Monte Rosa nappe in the Pennine Alps—A new working hypothesis. *Geological Society of America Bulletin, 113,* 604–614.

Glaciological reports, (1881–2017). *The Swiss Glaciers*, Yearbooks of the Cryospheric Commission of the Swiss Academy of Sciences (SCNAT) published since 1964 by the Laboratory of Hydraulics,

Hydrology and Glaciology (VAW) of ETH Zürich. No. 1–136. http://www.glamos.ch.

Gosse, J. C., & Phillips, F. M. (2001). Terrestrial in situ cosmogenic nuclides: theory and application. *Quaternary Science Reviews, 20,* 1475–1560.

Graf, A. (2007). *Genese alpiner Seitenmoränen am Beispiel des Findelengletschers bei Zermatt (VS). Master Thesis*, Universität Bern, unpublished, 126 pp.

Haeberli, W., & Hohmann, R. (2008). *Climate, glaciers and permafrost in the Swiss Alps 2050: scenarios, consequences and recommendations*. In 9th International Conference on Permafrost, Fairbanks, Alaska, 29 June 2008–3 July 2008, 607–612.

Hajdas, I. (2008). Radiocarbon dating and its applications in Quaternary studies. *Eiszeitalter und Gegenwart Quaternary Science Journal, 57,* 2–24.

Heiri, O., Koinig, K. A., Spötl, C., Barrett, S., Brauer, A., Drescher-Schneider, R., et al. (2014). Palaeoclimate records 60–8 ka in the Austrian and Swiss Alps and their forelands. *Quaternary Science Reviews, 106,* 186–205.

Helama, S., Jones, P., & Briffa, K. (2017). Dark ages cold period: A literature review and directions for future research. *The Holocene, 20,* 1–12.

Heyman, J. (2014). Paleoglaciation of the Tibetan Plateau and surrounding mountains based on exposure ages and ELA depression estimates. *Quaternary Science Reviews, 91,* 30–41.

Hippe, K., Ivy-Ochs, S., Kober, F., Zasadni, J., Wieler, R., Wacker, L., et al. (2014). Chronology of Lateglacial ice flow reorganization and deglaciation in the Gotthard Pass area, Central Swiss Alps, based on cosmogenic Be-10 and in situ C-14. *Quaternary Geochronology, 19,* 14–26.

Holzhauser, H. (1995). Gletscherschwankungen innerhalb der letzten 3200 Jahre am Beispiel des grossen Aletsch- und des Gornergletschers. Neue Ergebnisse. In *Gletscher im ständigen Wandel* (pp. 101–123). vdf Hochschulverlag AG an der ETH Zürich.

Holzhauser, H. (2010). *Zur Geschichte des Gornergletschers ein Puzzle aus historischen Dokumenten und fossilen Hölzern aus dem Gletschervorfeld* (253 pp.). Bern: Geographisches Institut der Universität Bern.

Holzhauser, H., Magny, M., & Zumbühl, H. J. (2005). Glacier and lake-level variations in west-central Europe over the last 3500 years. *The Holocene, 15,* 789–801.

Hormes, A., Müller, B. U., & Schlüchter, C. (2001). The Alps with little ice: evidence for eight Holocene phases of reduced glacier extent in the Central Swiss Alps. *The Holocene, 11,* 255–265.

Ivy-Ochs, S. (1996). *The dating of rock surfaces using in situ produced ^{10}Be, ^{26}Al and ^{36}Cl, with examples from Antarctica and the Swiss Alps. Ph.D. dissertation*, ETH Zürich, Zürich, Switzerland, 210 pp.

Ivy-Ochs, S. (2015). Glacier variations in the European Alps at the end of the last glaciation. *Cuadernos de Investigación Geográfica, 41,* 295–315.

Ivy-Ochs, S., Kerschner, H., Maisch, M., Christl, M., Kubik, P. W., & Schlüchter, C. (2009). Latest Pleistocene and Holocene glacier variations in the European Alps. *Quaternary Science Reviews, 28,* 2137–2149.

Ivy-Ochs, S., & Kober, F. (2008). Surface exposure dating with cosmogenic nuclides. *Eiszeitalter und Gegenwart Quaternary Science Journal, 57,* 179–209.

Joerin, U. E., Nicolussi, K., Fischer, A., Stocker, T. F., & Schlüchter, C. (2008). Holocene optimum events inferred from subglacial sediments at Tschierva Glacier, Eastern Swiss Alps. *Quaternary Science Reviews, 27,* 337–350.

Joerin, U. E., Stocker, T. F., & Schlüchter, C. (2006). Multicentury glacier fluctuations in the Swiss Alps during the Holocene. *The Holocene, 16,* 697–704.

Jörg, P. C., Morsdorf, F., & Zemp, M. (2012). Uncertainty assessment of multi-temporal airborne laser scanning data: A case study on an Alpine glacier. *Remote Sensing of Environment, 127,* 118–129.

Julen, K., & Taugwalder, R. (1995). *Orts- und Flurnamen der Gemeinde Zermatt* (p. 256). Zermatt: Gemeindebibliothek.

Kelly, M. A., Kubik, P. W., Von Blanckenburg, F., & Schlüchter, C. (2004). Surface exposure dating of the Great Aletsch Glacier Egesen moraine system, western Swiss Alps, using the cosmogenic nuclide 10Be. *Journal of Quaternary Science, 19,* 431–441.

Kerschner, H. (2009). Gletscher und Klima im Alpinen Spätglazial und frühen Holozän. In *Klimawandel in Österreich. Die letzten 20,000 Jahre und ein Blick voraus* (pp. 3–26). Innsbruck University Press.

Kerschner, H., & Ivy-Ochs, S. (2008). Paleoclimate from glaciers: Examples from the Eastern Alps during the Alpine Lateglacial and early Holocene. *Global and Planetary Change, 60,* 58–71.

Le Roy, M., Nicolussi, K., Deline, P., Astrade, L., Edouard, J.-L., Miramont, C., et al. (2015). Calendar-dated glacier variations in the western European Alps during the Neoglacial: the Mer de Glace record, Mont Blanc massif. *Quaternary Science Reviews, 108,* 1–22.

Lüthi, M. P. (2014). Little Ice Age climate reconstruction from ensemble reanalysis of Alpine glacier fluctuations. *Cryosphere, 8,* 639–650.

Madella, A. (2013). *Analysis of flute-forming conditions in Alpine setting: glacial bedforms at Findelengletscher*. Zermatt, Switzerland. *Master Thesis*, Universität Bern, unpublished, 27 pp.

Maisch, M., Haeberli, W., Frauenfelder, R., Kääb, A., & Rothenbühler, C. (2003). Lateglacial and Holocene evolution of glaciers and permafrost in the Val Muragl, Upper Engadin, Swiss Alps. *Permafrost, 2,* 717–722.

Maisch, M., Wipf, A., Denneler, B., Battaglia, J., & Benz, C. (1999). *Die Gletscher der Schweizer Alpen. Gletscherhochstand 1850, Aktuelle Vergletscherung, Gletscherschwund-Szenarien* (p. 373). Zürich: vdf Hochschulverlag ETH Zürich.

Mayr, F., & Heuberger, H. (1968). *Type areas of Lateglacial and postglacial deposits in Tyrol, Eastern Alps*. In: VII INQUA Congress, 143–165.

Menounos, B., Osborn, G., Clague, J. J., & Luckman, B. H. (2009). Latest Pleistocene and Holocene glacier fluctuations in western Canada. *Quaternary Science Reviews, 28,* 2049–2074.

Moran, A. P., Ochs, S. I., Vockenhuber, C., & Kerschner, H. (2016). Rock glacier development in the Northern Calcareous Alps at the Pleistocene-Holocene boundary. *Geomorphology, 273,* 178–188.

Nicolussi, K., Kaufmann, M., Patzelt, G., van der Plicht, J., & Thurner, A. (2005). Holocene tree-line variability in the Kauner Valley, Central Eastern Alps, indicated by dendrochronological analysis of living trees and subfossil logs. *Vegetation History and Archaeobotany, 14,* 221–234.

Nicolussi, K., & Patzelt, G. (2000a). Untersuchungen zur holozanen Gletscherentwicklung von Pasterze und Gepatschferner (Ostalpen). *Zeitschrift fur Gletscherkunde und Glazialgeologie, 36,* 1–88.

Nicolussi, K., & Patzelt, G. (2000b). Discovery of early Holocene wood and peat on the forefield of the Pasterze Glacier, Eastern Alps, Austria. *The Holocene, 10,* 191–199.

Nicolussi, K., & Schlüchter, C. (2012). The 8.2 ka event-Calendar-dated glacier response in the Alps. *Geology, 40,* 819–822.

Nishiizumi, K., Imamura, M., Caffee, M. W., Southon, J. R., Finkel, R. C., & McAninch, J. (2007). Absolute calibration of ^{10}Be AMS standards. *Nuclear Instruments & Methods in Physics Research, Section B: Beam Interactions with Materials and Atoms, 258,* 403–413.

Patzelt, G. (1977). Der zeitliche Ablauf und das Aussmass Postglazialer Klimaschwankungen in den Alpen. In Frenzel, B. (Ed.), *Dendrochronologie und Postglaziale Klimaschwankungen in Europa* (pp. 249-259). Volume 13, Erdwissenschaftliche Forschung.

Patzelt, G., & Bortenschlager, S. (1973). Die postglazialen Gletscher- und Klimaschwankungen in der Venedigergruppe (Hohe Tauern, Ostalpen). *Zeitschrift für Geomorphologie, Supplement, 16,* 25–72.

Paul, F., Machguth, H., Hoelzle, M., Salzmann, N., Haeberli, W. (2008). Alpine-wide distributed glacier mass balance modelling: a tool for assessing future glacier change? In Orlove, B. S., Wiegandt, E., and Luckman, B. H. (Ed.), *Darkening peaks: glacier retreat, science, and society* (pp. 111-125). Volume 2: Berkeley, University of California Press.

Pleuger, J., Froitzheim, N., & Jansen, E. (2005). Folded continental and oceanic nappes on the southern side of Monte Rosa (western Alps, Italy): Anatomy of a double collision suture. *Tectonics, 24,* 1–22.

Rasmussen, S. O., Andersen, K. K., Svensson, A. M., Steffensen, J. P., Vinther, B. M., Clausen, H. B., et al. (2006). A new Greenland ice core chronology for the last glacial termination. *Journal of Geophysical Research*. https://doi.org/10.1029/2005JD006079.

Rastner, P., Joerg, P. C., Huss, M., & Zemp, M. (2016). Historical analysis and visualization of the retreat of Findelengletscher, Switzerland, 1859–2010. *Global and Planetary Change, 145,* 67–77.

Reimer, P. J., Bard, E., Bayliss, A., Beck, J. W., Blackwell, P. G., Ramsey, C. B., et al. (2013). Intcal13 and Marine13 Radiocarbon Age Calibration Curves 0–50,000 Years Cal Bp. *Radiocarbon, 55,* 1869–1887.

Renssen, H., Seppä, H., Heiri, O., Roche, D. M., Goosse, H., & Fichefet, T. (2009). The spatial and temporal complexity of the Holocene thermal maximum. *Nature Geoscience, 2,* 411.

Schimmelpfennig, I., Schaefer, J. M., Akçar, N., Ivy-Ochs, S., Finkel, R. C., & Schlüchter, C. (2012). Holocene glacier culminations in the Western Alps and their hemispheric relevance. *Geology, 40,* 891–894.

Schimmelpfennig, I., Schaefer, J. M., Akcar, N., Koffman, T., Ivy-Ochs, S., Schwartz, R., et al. (2014). A chronology of Holocene and Little Ice Age glacier culminations of the Steingletscher, Central Alps, Switzerland, based on high-sensitivity beryllium-10 moraine dating. *Earth and Planetary Science Letters, 393,* 220–230.

Schneebeli, W., & Röthlisberger, F. (1976). *8000 Jahre Walliser Gletschergeschichte ein Beitrag zur Erforschung des Klimaverlaufs in der Nacheiszeit. Ph.D. dissertation*, University of Zürich, Verlag Schweizer Alpen-Club, Bern, Switzerland, 152 pp.

Seppä, H., Bjune, A. E., Telford, R. J., Birks, H. J. B., & Veski, S. (2009). Last nine-thousand years of temperature variability in Northern Europe. *Climate of the Past, 5,* 523–535.

Solomina, O. N., Bradley, R. S., Hodgson, D. A., Ivy-Ochs, S., Jomelli, V., Mackintosh, A. N., et al. (2015). Holocene glacier fluctuations. *Quaternary Science Reviews, 111,* 9–34.

Swindles, G. T., Plunkett, G., & Roe, H. M. (2007). A delayed climatic response to solar forcing at 2800 cal. BP: multiproxy evidence from three Irish peatlands. *The Holocene, 17,* 177–182.

Synal, H. A., Stocker, M., & Suter, M. (2007). MICADAS: A new compact radiocarbon AMS system. *Nuclear Instruments & Methods in Physics Research Section B-Beam Interactions with Materials and Atoms, 259,* 7–13.

von Grafenstein, U., Erlenkeuser, H., Brauer, A., Jouzel, J., & Johnsen, S. J. (1999). A mid-European decadal isotope-climate record from 15,500 to 5000 years BP. *Science, 284,* 1654–1657.

von Grafenstein, U., Erlenkeuser, H., Muller, J., Jouzel, J., & Johnsen, S. (1998). The cold event 8200 years ago documented in oxygen isotope records of precipitation in Europe and Greenland. *Climate Dynamics, 14,* 73–81.

Wacker, L., Nemec, M., & Bourquin, J. (2010). A revolutionary graphitisation system: Fully automated, compact and simple. *Nuclear Instruments & Methods in Physics Research Section B-Beam Interactions with Materials and Atoms, 268,* 931–934.

Wang, S., Ge, Q., Wang, F., Wen, X., & Huang, J. (2013). Abrupt climate changes of Holocene. *Chinese Geographical Science, 23,* 1–12.

Wanner, H., Solomina, O., Grosjean, M., Ritz, S. P., & Jetel, M. (2011). Structure and origin of Holocene cold events. *Quaternary Science Reviews, 30,* 3109–3123.

WGMS, (2015). Fluctuations of Glaciers 2005–2010. In Zemp, M., Frey, H., Gärtner-Roer, I., Nussbaumer, S.U., Hoelzle, M., Paul, F., Haeberli, W. (Ed.), ICSU (WDS)/IUGG (IACS)/UNEP/UNESCO/WMO: World Glacier Monitoring Service, Zurich, Switzerland:, Publication based on database version: https://doi.org/10.5904/wgms-fog-2012-11, p. 336.

Wiles, G. C., Lawson, D. E., Lyon, E., Wiesenberg, N., & D'Arrigo, R. D. (2011). Tree-ring dates on two pre-Little Ice Age advances in Glacier Bay National Park and Preserve, Alaska, USA. *Quaternary Research, 76,* 190–195.

Winistörfer, J. (1977). Paléogéographie des stades glaciaires des vallées de la rive gauche du Rhône entre Viège et Aproz (VS). *Bulletin de la Murithienne, 94,* 3–66.

Wipf, A. (2001). Gletschergeschichtliche Untersuchungen im spät- und postglazialen Bereich des Hinteren Lauterbrunnentals (Berner Oberland, Schweiz). *Geographica Helvetica, 56,* 133–144.

Wirsig, C., Ivy-Ochs, S., Reitner, J. M., Christl, M., Vockenhuber, C., Bichler, M., et al. (2017). Subglacial abrasion rates at Goldbergkees, Hohe Tauern, Austria, determined from cosmogenic ^{10}Be and ^{36}Cl concentrations. *Earth Surface Processes and Landforms, 42,* 1119–1131.

Zoller, H., Schindler, C. M., & Röthlisberger, H. (1966). Postglaziale Gletscherstände und Klimaschwankungen im Gotthardmassiv und Vorderrheingebiet. *Verhandlungen der Naturforschungs Gesellschaft Basel, 77,* 97–164.

Zumbühl, H. J. (1980). *Die Schwankungen der Grindelwaldgletscher in den historischen Bild-und Schriftquellen des 12. bis 19. Jahrhunderts: ein Beitrag zur Gletschergeschichte und Erforschung des Alpenraumes. Denkschriften der Schweizerischen Naturforschenden Gesellschaft 92* (279 pp.). Basel: Birkhäuser.

Zweck, C., Zreda, M., & Desilets, D. (2013). Snow shielding factors for cosmogenic nuclide dating inferred from Monte Carlo neutron transport simulations. *Earth and Planetary Science Letters, 379,* 64–71.